

Improved Resistance to Intergranular Corrosion in the AZ31B Magnesium Alloy by Friction Stir Welding

W. Aperador^{1,*}, A. Delgado^{1,2}, F. Franco³

¹Department of Engineering, Universidad Militar Nueva Granada, Carrera 11 No. 101-80, Fax:+57(1) 6343200, Bogotá, Colombia.

²Escuela Colombiana de Ingeniería – Julio Garavito, Bogotá, Colombia.

³Ingeniería de Materiales, Universidad del Valle, Ciudad Universitaria Meléndez, Cali, Colombia.

*E-mail: g.ing.materiales@gmail.com

Received: 10 May 2013 / Accepted: 29 May 2013 / Published: 1 July 2013

In this work, we present the decreased susceptibility to intergranular corrosion in AZ31 magnesium alloys welded by friction agitation process, varying the rotation and advance speed. To induce the corrosion effect was used as electrolyte a solution of 30g of NaCl and 10 ml of concentrated HCl, monitoring of degradation analysis was performed using electrochemical impedance spectroscopy and potentiodynamic polarization curves Tafel. Moreover, microstructural analyzes were performed of the grain boundaries by means of metallographic microscope and scanning electron microscope. It was found that a higher relationship among forward speed / rotation speed produces a weld bead with improved resistance to intergranular corrosion, possibly associated to a larger grain size in the stirred zone, in turn related to increased heat input by friction process.

Keywords: FSW, AZ31B magnesium alloy, intergranular corrosion.

1. INTRODUCTION

The magnesium alloys are a material that have been accepted widely by the industry automotive and aeronautical, due to its high mechanical resistance in relation with its low weight and low density; however for engineering applications, seldom the magnesium is used as a pure material which are added small percentages of aluminum, zinc and others to improve its mechanical properties; one of the commercial alloys frequently used is the AZ31 (nominally 3% Al, 1% Zn and 0,5 % Mn; Mg balance in weight percent [1-2]).

When it is required welding these alloys for some application using the traditional process of welding by fusion, problems and welding defects come up that are reflected in poor mechanical

properties, linked to microstructural changes which are produced by effects of the given thermal process [3-4]. As an innovative alternative, has been applied with better metallurgical and mechanical results the process of welding by friction stir (SFA). The SFA welding is a process of solid state union developed at 1991, in which the material throughout the welding is plastically deformed (moved, agitated) and heated by the rotation of a non consumable tool. This process generates a unique structure and different of the observed in the conventional methods of welding by fusion; which does not present fusion, is environmentally friendly and useful to join different alloys [5-8].

The magnesium alloys in comparison with materials as the aluminum or the steel present an electrochemical potential more negative, which make them more susceptible to corrosive phenomena from thermodynamic standpoint. The magnesium exposes good oxidation resistance in dry environments at room temperature. Nevertheless, the corrosion susceptibility is increased with the relative humidity and the temperature [9-11].

The reason for the low corrosion resistance of the magnesium alloys mainly is due to the following mechanisms i) the formed oxide films over the surface are not perfect or protective ii) the galvanic corrosion or bimetallic can be caused by impurities and secondary phases. Recently a variety of studies about the corrosion behavior of the Mg alloys have been performed; however, researches about corrosion of welding by friction in magnesium alloys are limited in the literature. [12-13]

The intergranular corrosion (IGC) occurs in the grain boundaries due to secondary phases precipitation. The grain boundaries are always the preferred sites where the precipitation and the segregation in the alloy occur. It is consider that the alloys with intermetallic phases or compound are highly susceptible to intergranular corrosion.

In this work is determinated the proper relations among the lineal velocity and the rotation velocity to decrease the intergranular corrosion susceptibility that suffers the magnesium alloys AZ31B welded by the friction stir process, the evaluation was performed by electrochemical techniques and immersion in a solution composed of 30g NaCl and 10ml HCl concentrate per liter.

2. EXPERIMENTAL DETAILS

Table 1. Chemical composition of AZ31B

Al	2.5 a 3.5
Mn	0.20 min.
Zn	0.60 1.4
Ca	0.04 max.
Si	0.10 max.
Cu	0.05 max.
Ni	0.005 max.
Fe	0.005 max.
Others	0.30 max.

Laminate of AZ31B magnesium alloy were used; they were cut from hot extruded profiles, with dimensions of 90 x 120 x 3.2 mm of thin. The chemical composition of the base material obtained by fluorescence analysis is presented in the table 1.

The plaques were cut at a longitude of 160 mm x 80 mm of width for the execution of the weld beads. The SFA process was performed using a universal milling machine, Conditioning for this purpose, as shown in figure 1. The specimens were made at different conditions of rotation velocity and welding velocity, keeping constant the penetration and the tool inclination, as shown in table 2.



Figure 1. Scheme of the used mounting in the welding process SFA.

Table 2. Variables of SFA process

Rotation velocity (rpm)	1800 y 900
Forward velocity (mm/min)	250, 125,160 y 80
Tool inclination(°)	1
Tool penetration (mm)	2,9

For the intergranular corrosion test, after the plaques were welded, they were cut transversely to the weld seam with a width of 15 mm. Then the plaques were polished with different sandpapers (1801500), and polished in the cloths of 1.3 and 0.05 μm , using for the first two diamond paste and the last one alumina of 0.05 μm . Subsequently, the specimens were immersed in an acid solution with a pH of 3.6 composed by 0.5 M of NaCl and 0.001 of HCl, the samples were immersed during 24 hours later on were washed and dried. The intergranular corrosion susceptibility was evaluated by visual inspection of the material cross-sections, for record of the IGC was used a metallographic optical microscope Olympus DP72 and a scanning electron microscope Philips XL 30 FEG of high resolution.

The electrochemical tests were performed with immersion of the samples in acid solution composed by 0.5 NaCl and 0.001 M of HCl. The reference electrode type used in all test was an Ag/AgCl electrode of analytical type Electrochemistry BAS (MF-2052 RE-5B), which has a potential

of +0.235 V respect to the reference electrode of hydrogen at 25°C. All the potentials are referenced to the potential of the Ag/AgCl electrode. In the potentiostatic and impedance spectroscopy tests was used an auxiliary electrode of platinum. The working temperatura of the tests was 25°C, controlled with an oscillation of $\pm 0.1^\circ$ C. To avoid the contamination of the working medium, the used specimens and electrodes both were cleaned with bidistilled water and were dried at air before were immersed in the fluid. For the intergranular corrosion evaluation in static conditions was used a potentiostat – galvanostat PCI-4 model. The specimens were analyzed through the electrochemical impedance spectroscopy techniques (EIS) and Tafel polarization curves. The Nyquist diagrams were obtained by the frequency sweeps in the range of 0,001 Hz to 100 kHz, using amplitude of the sinusoidal signal of 10 mV. The Tafel diagrams were obtained at a scan velocity of 0.125 mV/s in a voltage range -0.25V to 0.6V with an exposed area of 1 cm².

The equivalent circuits showed were performed by simulations with non-linear adjustment through the Gamry software in order to adjust the obtained data. The main parameter obtained by impedance spectroscopy has been the transference resistance of the loads of the studied specimens. From the calculated parameters by simulation, were calculated the transference resistances for all the specimens.

3. RESULTS AND ANALYSIS

3.1 Electrochemical analysis

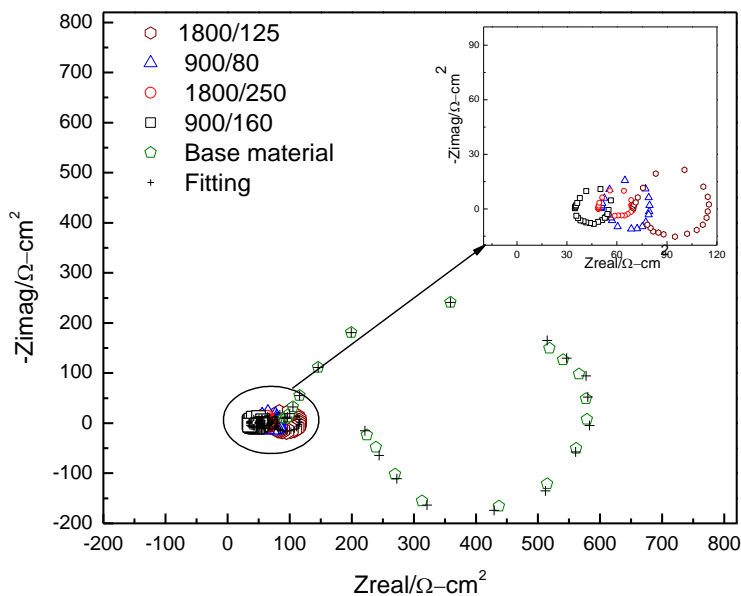


Figure 2. Nyquist diagram of the AZ31B alloy, welded by the friction stir process modifying the rotation velocity and forward velocity parameters.

In the figure 2, is shown the Nyquist diagrams corresponding to the AZ31B alloys, welding by friction stir process. For the welds that were worked with rotation velocity/forward velocity relations (V_r/V_a) 1800/125 and 900/80, were generated the greatest total impedance values; that for the obtained at 1800/125 and 900/160. It is due to the phenomenon of velocity decreased, which affects the mechanism as a consequence of the influence of the process parameters in the microstructure of the magnesium alloys welded by friction stir, furthermore owing to the recrystallized grains size which diminish with a decrease in the rotation velocity for a forward velocity constant or diminish.

In the figure 3, it was observed the equivalent circuit obtained for the welds, the elements that represent are directly related to the degradation phenomenon which suffered these specimens when are subjected to a aggressive medium, R1 correspond to solution resistance, R2 and CPE are elements that simulated the electrolyte interphase – protector layer of MgO, L and RL are associated to adsorption – desorption phenomena of species at the electrode surface, phenomena that alter the electrode potential and the corrosion velocity of the metal. The constant phase element CPE is used to adjust of the semicircle data that are present among the high and medium frequencies, this semicircle is due to dispersion in the time constant principally, caused by the irregularities in the magnesium surface, in general by process associated to the irregular distribution of the applied potential (10 mV), for obtaining EIS data.

In the table 3, is indicated the used parameters values in the simulation and the representation of the admittance of a CPE, showing a depended energy fraction of the angular frequency, $Y_{CPE} = Y_P (j\omega)^\alpha$. Additionally, in the Nyquist diagram of the figure 2, it is observed a inverted semicircle which is associated to a induction of low frequency. The values of inductance (L) that is adjusted to these data are in the range of the Henry, associated to the material response, indicating the presence of Mg + metastable during the dissolution of magnesium [14].

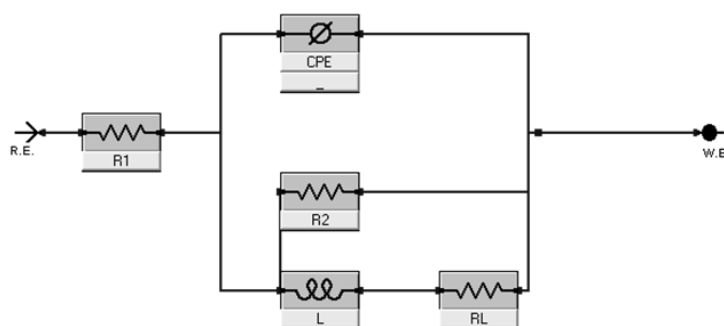


Figure 3. Equivalent circuit, corresponding to AZ31B alloy, welded by the process of friction stir, with the velocities 1800/125, 900/80, 1800/250, 900/160.

In the figure 4, it is observed the polarization curves for the four immersed welds in the aggressive solution; the evaluated specimens generated dissolution of general form in the anodic region [15]. In the polarization curves is appreciated that the relation of velocities denominated highs (1800/125 and 900/160), is obtained decrease in the corrosion potential and increase in the densities of

corrosion current. This response is related with the product of thermal and mechanical cycles due to the process which caused the modification of the surface.

Table 3. Values of the polarization curves of the welds obtained changing the parameters of rotation velocity and forward velocity.

rotation velocity/ forward velocity	R_1 $\Omega \text{ cm}^2$	Y_{CPE} $\text{F cm}^{-2} \text{ s}^{-(1-\alpha_1)}$	α_1	R_2 $\Omega \text{ cm}^2$	L H	R_L $\Omega \text{ cm}^2$
90/160	35.21	19.21×10^{-6}	0.63	42.21	7.32	12.32
1800/250	48.42	49.66×10^{-6}	0.66	63.21	5.43	13.21
900/80	51.28	67.34×10^{-6}	0.91	90.45	10.21	21.48
1800/125	70.21	93.09×10^{-6}	0.93	120.34	19.26	35.43

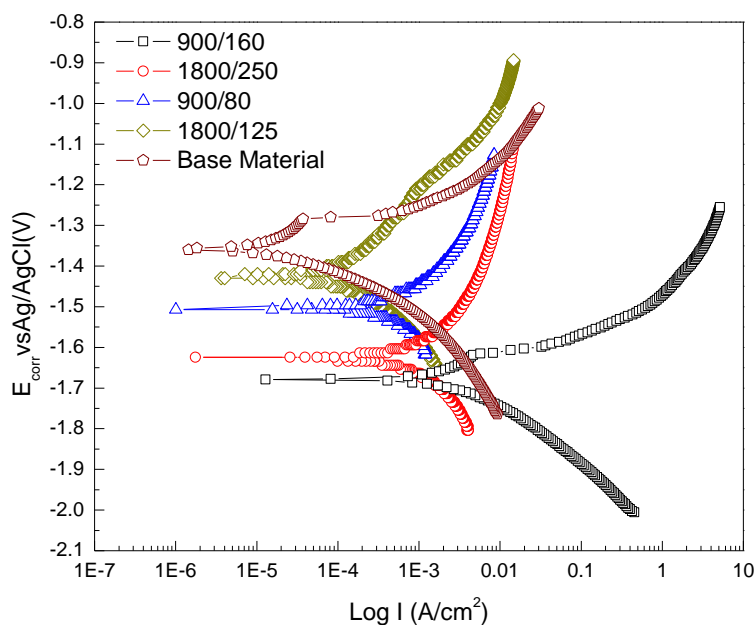


Figure 4. Polarization curves of the AZ31B alloy, welded by the process of friction stir, modifying the parameters of rotation velocity and forward velocity.

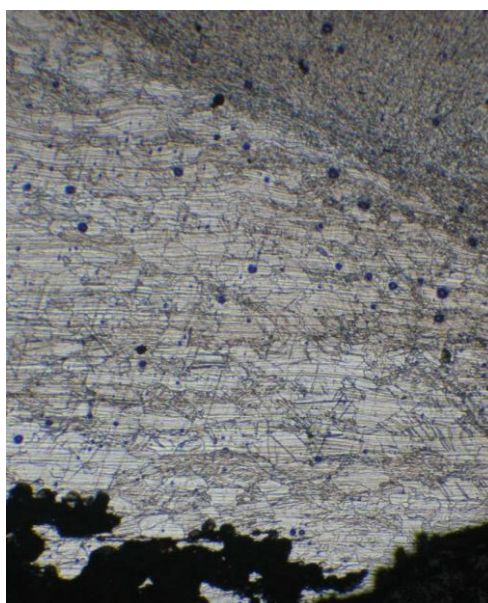
In the table 4, it is shown the polarization curves values in a region of $\pm 250\text{mV}$ close to the corrosion potential of each one of the welds, obtaining similar values of density and velocity of corrosion for the welds with high value of velocity relation, moreover by decrease this relation is evidenced an high increase of the corrosion velocity, this supports what is observed in the technique of electrochemical impedance spectroscopy, where the total impedance of the system is similar for the relation of high velocities (1800/125 and 900/80), and small for low velocity (1800/250 and 900/160).

Table 4. Polarization curves values of the welds obtained changing the parameters of rotation velocity and forward velocity.

	Anodic slope /mV-decade	Cathodic slope/mV-decade	Corrosion current/ $\mu\text{A cm}^{-2}$	Corrosion potential /mV	Corrosion velocity / mpy
Base material	67	91	81.9	-1893	43.9
1800/125	-135	-65	179	-1421	255
900/80	-45	-95	669	-1492	955
1800/250	112	254	1070	-1628	1527
900/160	289	269	4660	-1673	6654

3.2 Microstructural analysis

Subsequently of the corrosion accelerated test and removing the corrosion products, in the welds is observed pitting corrosion over the zone where is the base metal, a dissolution process more intense is appreciable at the bottom (in the weld bead), as shown in the figure 5, this susceptibility difference to the corrosion is due to the thermal cycle produced in the weld and the strong deformation experienced by the material during the process, the different zones that are presented cause a potential difference which is the driving force for the initiation of the dissolution process, owing to the bottom part which is a narrower zone into a cone shape, this behaves in anodic mode respect to the sides that are base material which act in cathodic manner, generating a cell where is seen the area effect since the base material zones are greater than this small zone, by the presence of the chloride ion, the attack is greatly intensified and continues in this direction. Conversely to the shape of the weld bead in the interior (dark zone).

**Figure 5.** Micrograph of the zone corresponding to weld by the friction stir process.

In the figure 6a and 6b is observed small traces of dissolution, this initiated and propagated through the grain boundaries (by the greater activity of these) and in the zone of greater deformation (agitated zone); being present a greater amount of solution or humidity and due to the high activity of the magnesium, its dissolution is propagated through the interior of the grains, this corrosion type attack along the grain boundary and form deep and narrow paths.

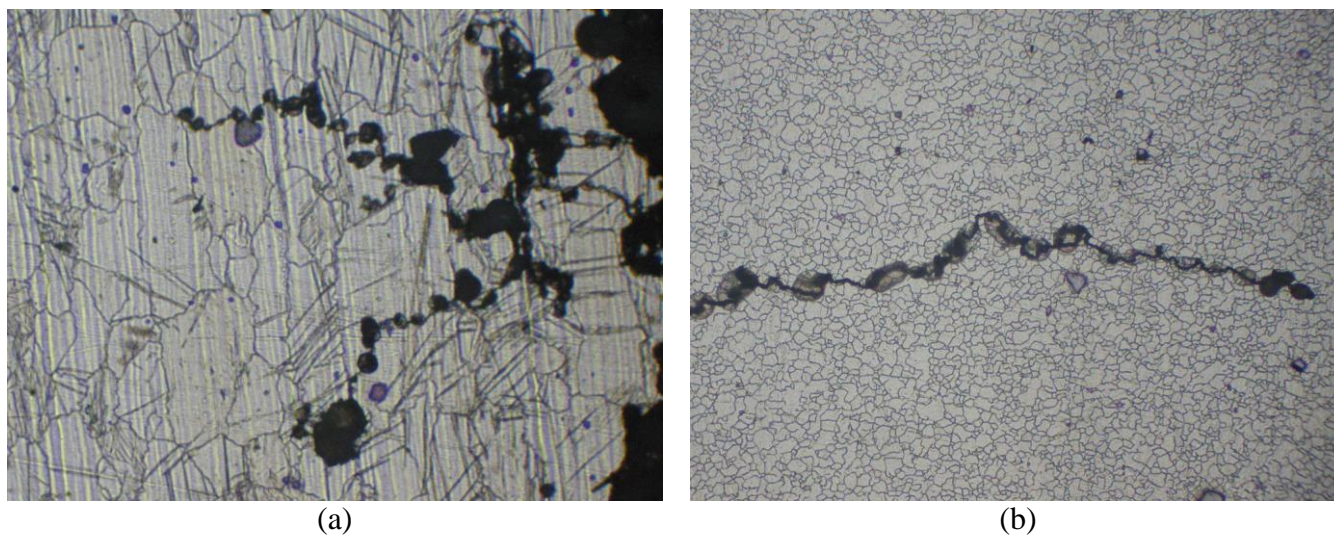
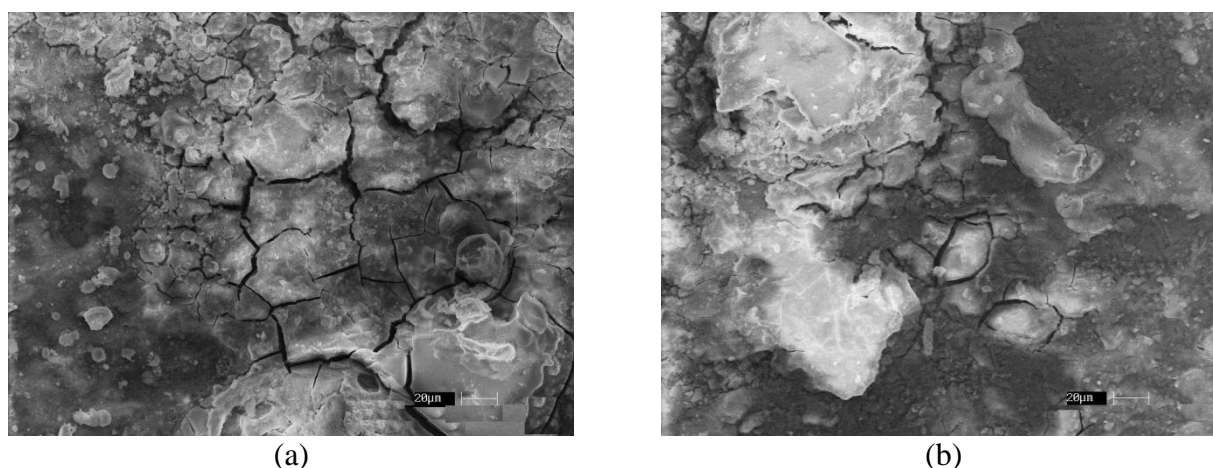


Figure 6. Micrograph a) observation of the grain limit and beginning of the intergranular corrosion, b) propagation of the corrosion through the grain limits.

In the figure 7 is observed the scanning electron microscopy, made over the surfaces of Mg alloys, after have been subjected to the process of electrochemical evaluation. It can be observed in all the specimens a film that presents cracks, which is not compact and fully heterogeneous, these cracks are associated with the intergranular corrosion, given that at higher velocity reaction is obtained a increase in the size of the grain, generating greater corrosion products (figure 7c and 7d), and for low velocities (1800/250 and 900/160) the heat entrance is less mitigating the grain size growth and generating less quantity of corrosion products (figure 7c and 7d).



(a)

(b)

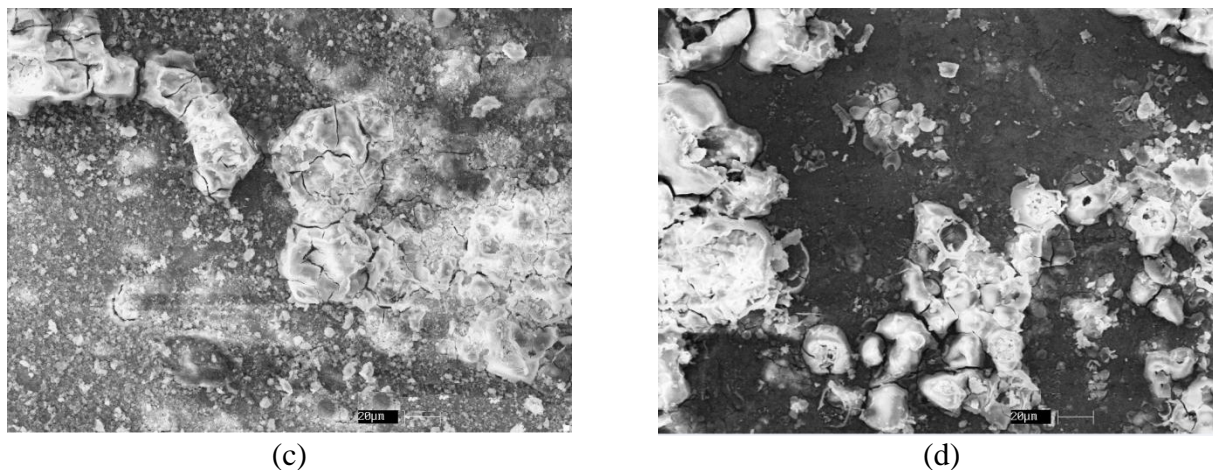


Figure 7. MEB micrographs of corrosion products deposited in the Mg surface with the following relations of rotation velocity/forward velocity a) 1800/125 b) 900/80 c) 1800/250 and d) 900/160.

4. CONCLUSIONS

In the AZ31B alloy was evidenced that the corrosion occurs first in superficial effects as grain limits, furthermore the oxide film or passive film is susceptible to nuclear in the crystalline defects.

According to the obtained results for the welds that were worked with relation (V_r/V_a) 900/160 and 1800/250, were calculated higher corrosion velocities than for the worked at 900/80 and 1800/125, because during the welding process by friction stir is produced in the central zone a dynamic recrystallization producing fine grains, this recrystallized grain size decreases with a decline in the relation rotation velocity/ forward velocity.

ACKNOWLEDGEMENTS

The authors acknowledge the at the Universidad Militar Nueva Granada

References

1. ASM-American Society for Metals Metal Handbook v.2. Properties and Selection: Nonferrous Alloys and Special-Purpose Materials, 10^a. Ed. Metal Park- Ohio, p 3298, 1992.
2. W. Aperador, G. Rodríguez, F. Franco. *Ingeniare. Revista chilena de ingeniería*, 20 (2012) 119
3. F. Franco, H. Sánchez, D. Betancourt, O. Murillo. *Revista Latinoamericana de Metalurgia y Materiales*, S1 (2009) 1369
4. G. Padmanaban, V. Balasubramanian. *Materials and Design*, 3 (2010) 3724
5. M. Amú, F. Franco. *Revista Latinoamericana de Metalurgia y Materiales*, S1 (2009) 767
6. S.M Chowdhury, D.L Chen, S. D Bhole, X. Cao, E. Powidajko, D. C Weckman, Y. Zhou. *Materials Science and Engineering A*, 527 (2010) 2951
7. S. Gang, L. Liming, W. Peichong. *Materials Science and Engineering*, 429 (2006) 312
8. J. Chen, H. Fujii, Y. Sun, Y. Morisada, K. Kondoh, K. Hashimoto. *Materials Science and Engineering: A*, 549 (2012) 176

9. R.C Zeng, J. Chen, W. Dietzel, R. Zettler, J. dos Santos, M. Lucia Nascimento, K. Ulrich. *Corrosion Science*, 51 (2009) 1738
10. M. Bobby Kannan, W. Dietzel, R. Zeng, R. Zettler, J.F dos Santos. *Materials Science and Engineering A*, 460–461 (2007) 243
11. S. Ramesh Babu, V.S Senthil Kumar, G. Madhusudhan, L. Karunamoorthy. *Procedia Engineering*, 38 (2012) 2956
12. M.A Mofid, A. Abdollah-Zadeh, F. Malek Ghaini. *Materials & Design*, 36 (2012) 161
13. Y. L Cheng, H.I Wu, Z. H. Chen, H.M Wang, Z. Zhang, Y.W Wu. *Transactions of Nonferrous Metals Society of China*. 2007; 17 (3): 502-508.
14. M. Zaharescu, L. Predoana, A. Barau, D. Raps, F. Gammel, N.C Rosero-Navarro, Y. Castro, A. Durán, M. Aparicio. *Corrosion Science*. 51 (2009) 1998
15. Q. Qu, J. Ma, L. Wang, L. Li, W. Bai, Z. Ding. *Corrosion Science*. 53 (2011) 1186